PAPER • **OPEN ACCESS**

Design and experimental performances of a piezoelectric stick-slip actuator for rotary motion

To cite this article: Zhaochen Ding *et al* 2019 *IOP Conf. Ser.: Mater. Sci. Eng.* **563** 042068

IOP Conf. Series: Materials Science and Engineering **563** (2019) 042068 doi:10.1088/1757-899X/563/4/042068

Design and experimental performances of a piezoelectric stick-slip actuator for rotary motion

Zhaochen Ding[1], Jingshi Dong[1*], Haojie Yin[1], Zhe Wang[1], Xiaoqin Zhou[1] and Zhi Xu[1]

[1]School of mechanical and aerospace engineering, Jilin University, Changchun 130022, China

[*]Corresponding author: Jingshi Dong(e-mail: dongjs@jlu.edu.cn)

Abstract. In order to reduce the regression phenomenon of the piezoelectric stick-slip actuator, and improve the output performance, a piezoelectric stick-slip actuator with regular octagonal flexible hinge mechanism is proposed in this paper. The pseudo-rigid body method is used to analyze the regular octagonal flexible hinge mechanism and the flexible driving foot respectively.A prototype is fabricated to test the working performance and the results demonstrate that the minimum step is 0.01μm, the maximum speed is 145251μrad/s, and the maximum load carrying capacity is 500g. The experimental results show that the parasitic motion suppresses the regression of the actuator and improves the output stability.

1. Introduction

In recent years, due to high resolution[1], fast response[2], , etc., piezoelectric actuators have been widely used in bio-medicine[4], ultra-precision machining[5], and other fields. According to the difference of the driving principle, the stepping piezoelectric actuator can be divided into ultrasonic, inchworm and piezoelectric stick-slip actuator, each of which has its own advantages and disadvantages. Ultrasonic actuator has the advantages of compact structure and fast movement speed and so on, but its energy consumption is high [6]; the efficiency of inchworm actuator is high, but its mechanical structure is complex and the movement speed is low [7].

Compared with the above mentioned piezoelectric actuators, the stick-slip actuator has higher kinematic precision and a simple mechanical structure. Existing stick-slip actuators, such as the piezoelectric stick-slip actuator developed by Paderborn University in 2013, used the resonance effect and the flexible hinge's amplification mechanism to increase the motor speed [8]. The piezoelectric actuator[9] designed by Li et al. in 2015 not only can realize high-resolution large-stroke linear displacement, but also can achieve the displacement in the x and y directions by using only one piezoelectric stack.

This paper introduces a piezoelectric stick-slip actuator through the parasitic motion of the regular octagonal flexible hinge, which can increase forward static friction and reduce the influence of sliding friction on motion [10].

2. The structure and working principle of actuator

2.1 The structure of actuator

The structure of the actuator is mainly composed of fixed base, annular rotor and stator, as shown in Fig 1 .The stator structure includes a piezoelectric stack, a regular octagonal flexible hinge mechanism, flexible drive feet, and flexible reset springs, as shown in Fig 2. The piezoelectric stack in the stator is embedded in the regular octagonal flexible hinge mechanism groove in a tight fit. The regular octagonal flexible hinge mechanism material selects the spring steel 65Mn.

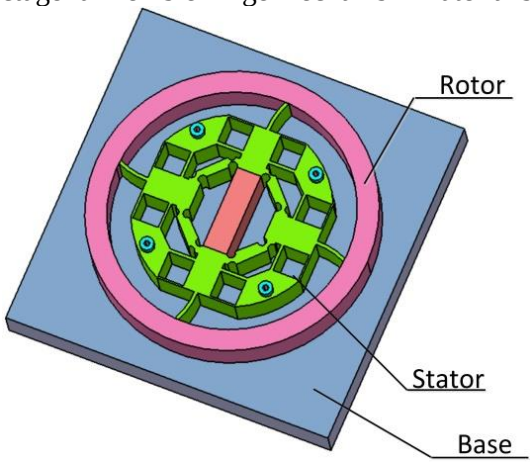

Fig 1. Parasitic piezoelectric stick slip actuator

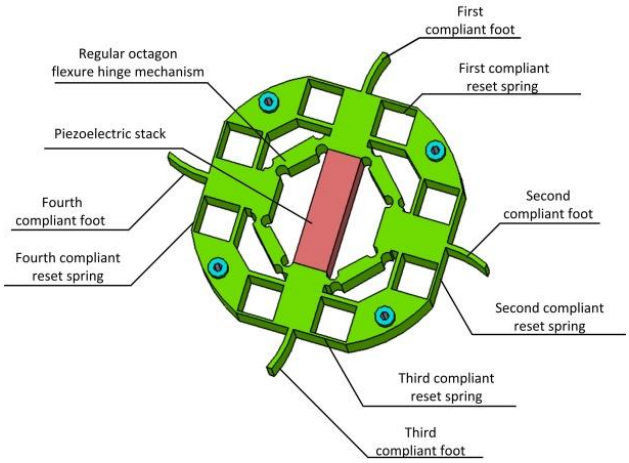

Fig 2. Structure diagram of the stator

2.2 The working principle of actuator

The working principle of the proposed piezoelectric stick-slip actuator is shown in Fig 3. Each kinematic cycle can be divided into two steps:

Step a: From t_0 to t_1, the input voltage rises slowly, the piezoelectric stack slowly elongates, the regular octagonal flexible hinge mechanism is slowly deformed, the first and third flexible reset springs are outwardly convex, and the second and fourth flexible reset spring is recessed inwardly such that the static friction between the first and third flexible driving feet and the contact point of the annular rotor is increased such that the annular rotor rotates clockwise by a slight angle $\Delta\alpha$.

Step b: From t_1 to t_2, the input voltage drops rapidly, the piezoelectric stack quickly retreats to the initial position, the first and third flexible reset springs are reset by the convex state, and the second and fourth flexible reset springs are reset by the recessed state, the pre-tightening force of the contact points between the second and fourth flexible driving feet with the annular rotor is increased, and the regression phenomenon of the annular rotor is reduced.

Repeat the two steps, the annular rotor can achieve large stroke rotary motion.

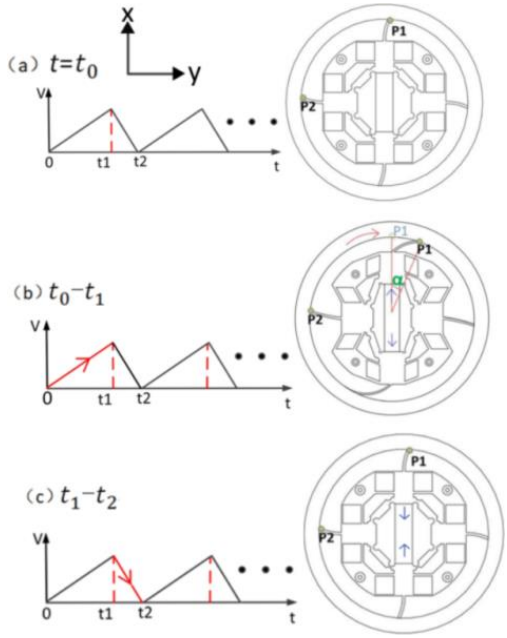

Fig 3. Working principle

3. Design and analysis

3.1 Design and calculation of regular octagonal flexible hinge

The designed pseudo rigid body model of regular octagonal flexible hinge is shown in Fig. 4(a). The regular octagonal flexible hinge mechanism is seen as a system connected by rigid rods, as shown in Fig 4(b). Point C is the point of contact between the flexible drive foot and the regular octagonal flexible hinge mechanism. The speeds of the three points A, B, and C on the regular octagonal flexible hinge mechanism can be expressed by the following formula:

$$v_A = \frac{\Delta x}{\Delta t} \quad (1)$$

$$v_B = \frac{\Delta y}{\Delta t} \quad (2)$$

$$v_C = v_B \quad (3)$$

When the rigid rod AB is rotated at an angular velocity around the rotation center O, the formulas (1), (2) can be expressed by the following formula:

$$v_A = \omega \cdot l_y \quad (4)$$

$$v_B = \omega \cdot l_x \quad (5)$$

Therefore, the regular octagonal flexible hinge mechanism magnification ratio Q can be obtained by the formula (6):

$$Q = \frac{\Delta x}{\Delta y} = \frac{v_A}{v_C} = \frac{v_A}{v_B} = \frac{\omega \cdot l_y}{\omega \cdot l_x} = \frac{l_{ab} \cdot \cos\alpha}{l_{ab} \cdot \sin\alpha} = \cot\alpha \quad (6)$$

Among them: α represents the angle between the y-axis and the rod AB; l_{ab} represents the length between the two points of AB.

Since the regular octagonal flexible hinge mechanism has a symmetrical structure, during the slow elongation phase of the piezoelectric stack, the displacement of the C point in the x direction can be calculated by the formula (7):

$$\Delta Cx = \Delta x = \Delta y \cdot Q = \Delta y \cot\alpha \quad (7)$$

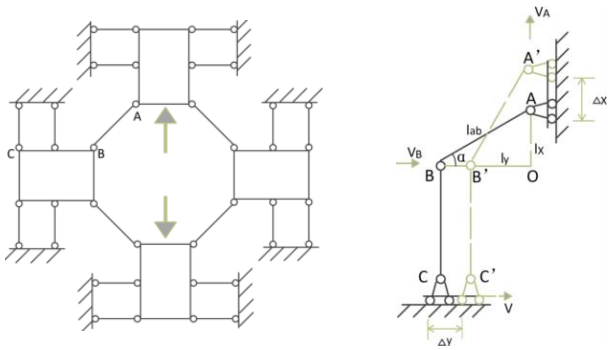

（a） （b）

Fig 4. Sketch of integral structure and structure of eight sided flexure hinge

3.2 Design and analysis of flexible driving feet

The moving path of the flexible driving foot is simulated by a torsion spring connecting with a pseudo rigid body, as shown in Fig 5.

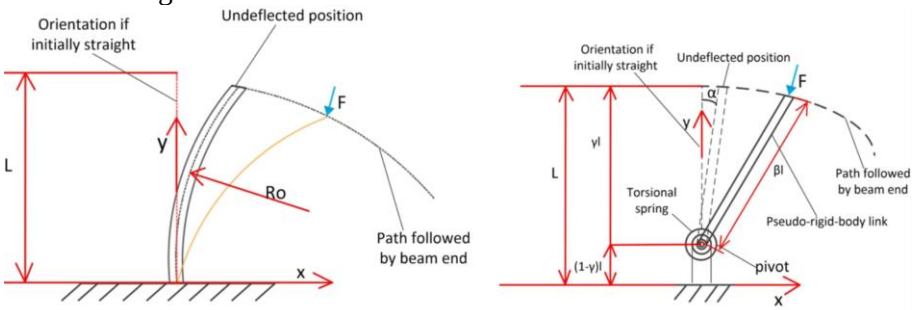

（a） （b）

Fig 5. Pseudo rigid body model with flexible driving foot

Among them, when the flexible driving foot moves, its curvature parameter can be expressed by the following formula [11]：

$$k_0 = \frac{l}{R_0} \approx 0.0417 \qquad (8)$$

At the same time, by looking up the table [12], you can get the following parameters:

γ=0.845； β=0.844。

4. Experiment and analysis

4.1 Build experiment test system

The prototype of the stick-slip actuator is manufactured by wire cutting. The stator diameter is Φ60mm and the thickness is 6mm. The material of the stator is 65Mn spring steel. The diameter of the annular rotor is Φ60mm and the thickness is 8mm.When the test system is working, the signal amplifier amplifies the sawtooth signal output from the signal generator and passes the laser displacement sensor to make relevant measurement.

4.2 Test and analysis of experiment

All experiments were performed using a saw-tooth signal with a duty cycle of 100%. The relationship between displacement and time is shown in Fig 6. In the same time, as the voltage rises, the displacement gradually increases. It is because when the driving voltage increases, the elongation of the piezoelectric stack gradually increases, thereby increase pre-tightening force and driving force of the contact point between the annular rotor and the flexible driving foot.

We also can see that each kinematic cycle can be divided into two phases: the forward motion phase and the backward motion phase, and the kinematic step distances are L and L_0 respectively. The regression is generated because the piezoelectric stack quickly retreats to the initial position when the saw-tooth waveform drops rapidly, and the sliding friction between the first and third flexible driving feet and the annular rotor is caused by the relative motion, thereby making the annular rotor generate regression. This regression phenomenon is an inherent characteristic of the stick-slip principle.

Therefore, the actual moving step of the annular rotor at each cycle is:

$$\Delta L = L - L_0 \tag{9}$$

Step angle of the annular rotor:

$$\Delta\theta \approx \frac{\Delta L}{R} \tag{10}$$

Among them, R is the radius of the annular rotor, and its value is 30 mm. The speed and rotation angle of the drive can be converted by this formula.

When the driving actuator is lower than 10 V, the actuator cannot work normally, so the starting voltage of the actuator is 10 V. At this time, the minimum step of the actuator is 0.01μm. According to formula (10), the minimum rotation angle of the actuator is 0.33μrad.

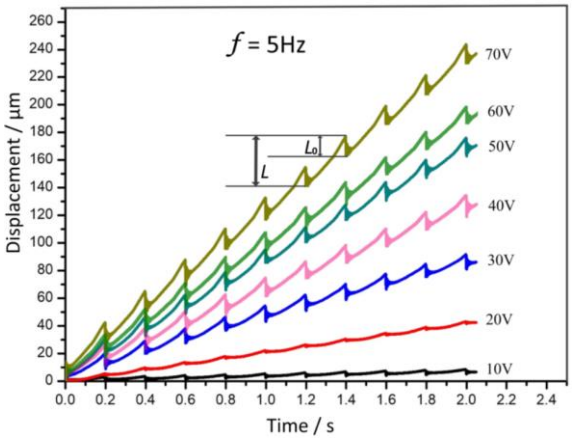

Fig 6. Relationship between displacement and time

When the input voltage is controlled at 70V, the relationship between the speed and frequency of the actuator is shown in Fig 7. As the frequency increases, the speed of the actuator increases, reaching a maximum value of 145251μrad/s at 900 Hz. There are two reasons for the speed drop: when the frequency is too high, the mechanical response of the flexible drive foot cannot keep up with the piezoelectric stack, or when the frequency is too high, the increase in power causes the drive device to fail to achieve the full motion of the piezoelectric stack.

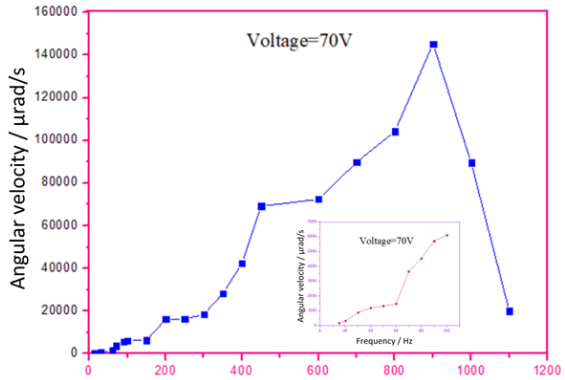

Fig 7. Relationship between angular velocity and frequency

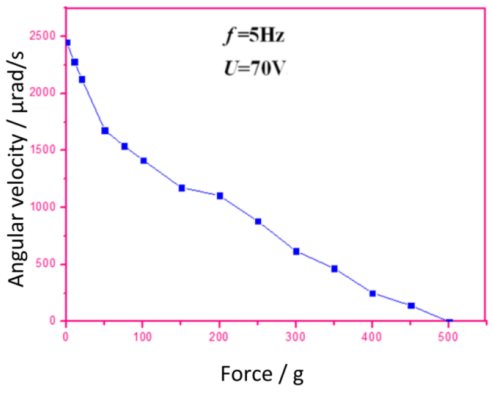

Fig 8. Relationship between angular velocity and vertical load

The standard weight is placed directly above the slider to measure the load-to-speed relationship of the piezoelectric stick-slip actuator, as shown in Fig 8. It can be seen that, at 5 Hz and 70 V, as the load increases, the speed of the annular rotor gradually decreases, and when the load weight exceeds 500 g, the piezoelectric actuator does not produce forward motion, so the maximum load carrying capacity of the actuator is 500 g.

5.Conclusion

In this paper, a piezoelectric stick-slip actuator is developed. The structure analysis shows that the actuator can increase forward static friction and reduce the influence of sliding friction on motion to decrease regression. When the driving frequency is 900 Hz and the driving voltage is 70 V, the maximum angular velocity is 145251μrad/s. When the driving voltage is 10 V, the minimum step is driven, the distance is 0.01μm. When the driving frequency is 5 Hz and the driving voltage is 70 V, the maximum load carrying capacity is 500 g. The results prove that the parasitic motion of the positive octagonal flexible hinge can improve the output stability.

References

[1] A. J. Fleming and K. K. Leang, Design, Modeling and Control of Nanopositioning Systems (Springer, 2014).
[2] Fleming A J and Leang K K 2014 Design, Modeling and Control of Nanopositioning Systems (Cham: Springer)
[3] Palosaari J, Leinonen M, Juuti J, Hannu J and Jantunen H 2014 Piezoelectric circular diaphragm with mechanically induced pre-stress for energy harvesting Smart Mater. Struct. 23 085025
[4] Dong Jingshi,Cheng Guangming,Shen Chuanliang,et al.Piezoelectric Insulin Pump[J].Journal of Xi'an Jiaotong University,2007,41(05):602-605
[5] Huang H, Lu F, Zhao H, et al. Note: A novel rotary actuator driven by only one piezoelectric actuator[J]. Review of Scientific Instruments, 2013, 84(9):121101.
[6] W. M. Kuo, S. F. Chuang, C. Y. Nian, and Y. S. Tarng, “Precision nanoalignment system using machine vision with motion controlled by piezoelectric motor,” Mechatronics, vol. 18, pp. 21–34, Feb. 2008.
[7] D. Kang, M. G. Lee, and D. Gweon, “Development of compact high precision linear piezoelectric stepping positioner with nanometer accuracy and large travel range,” Rev. Sci. Instrum., vol. 78, Jul. 2007, Art. 075112.
[8] Hunstig M, Hemsel T, Sextro W. Stick–slip and slip–slip operation of piezoelectric inertia drives. Part I: Ideal excitation[J]. Sensors & Actuators A Physical, 2013, 200(4):90-100.
[9] Li J, Zhou X, Zhao H, et al. Design and experimental performances of a piezoelectric linear actuator by means of lateral motion[J]. Smart Materials & Structures, 2015, 24(6).
[10] Cheng T, He M, Li H, et al. A Novel Trapezoid-Type Stick-Slip Piezoelectric Linear Actuator Using Right Circular Flexure Hinge Mechanism[J]. IEEE Transactions on Industrial Electronics, 2017, PP(99):1-1.
[11] Wang S, Rong W, Wang L, et al. Design, analysis and experimental performance of a piezoelectric rotary actuator based on compliant foot driving[J]. Microsystem Technologies, 2017, 23(8):1-9.
[12] Howell LL, Magleby SP, Olsen BM (2013) Handbook of compliant mechanisms.Wiley, Hoboken